ChemComm
Chemical Communications

This article can be cited before page numbers have been issued, to do this please use: J. C. Izang and J. R. Bour, *Chem. Commun.*, 2026, DOI: 10.1039/D6CC02735K.

ChemComm

View Article Online
DOI: 10.1039/D6CC02735K

COMMUNICATION

Identification of an Air- and Moisture-Tolerant MOF-Based C–H Amination Catalyst

John C. Izang [a] and James R. Bour,*[a]

Received 00th January 20xx,
Accepted 00th January 20xx

DOI: 10.1039/x0xx00000x

PCN-222(Co), a mesoporous Zr-based cobalt-porphyrin MOF, catalyzes benzylic C–H amination under air, with added water, and with limiting C–H substrate. Direct comparison to molecular Co-porphyrins implicates a protective framework microenvironment, rather than linker electronics, as the origin of this air and water tolerance.

Direct conversion of C–H bonds into C–N bonds is a longstanding objective in the synthesis of organic amines because it bypasses prefunctionalized substrates to access valuable amine products.[1–4] Among the available strategies, nitrene transfer from organic azides is especially attractive, and Co^{II} metalloradical porphyrins are particularly effective catalysts for this transformation.[5–17] They combine low cost with high activity and excellent selectivity across a wide range of weak C–H bonds. The development of these catalysts represents a significant advance but a practical limitation remains: most high-performing systems generally require rigorously inert, anhydrous conditions. At least three deactivation pathways under such conditions have been invoked, including bimolecular decomposition of Co^{III}–nitrene radical intermediates, oxidation by O_2, and/or axial coordination of H_2O at cobalt.[18–21]

Porphyrin metal–organic frameworks provide an attractive platform for stabilizing reactive intermediates and directing substrate-catalyst interactions to help overcome deactivation limitations.[22,23] Incorporating the porphyrin as a structural linker limits bimolecular catalyst interactions without the typical steric bulk required to avoid similar interactions in molecular analogues. In addition, the polarity, substrate partitioning, and effective water activity within MOF pores can differ substantially from the bulk medium.[24,25] Taken together, these effects and others often augment the activity and stability of catalytic centers confined in MOFs relative to their solution counterparts.[26–29] Consistent with these observations, heterogenized metalloporphyrins have shown enhanced robustness in several catalytic contexts,[30,31] and porphyrinic MOFs have been widely applied in oxidation, CO_2 reduction, and photocatalysis.[32–35] Their use in nitrene-transfer catalysis, however, remains comparatively limited. More importantly, to our knowledge, no study has directly tested whether embedding a cobalt porphyrin nitrene-transfer catalyst within a porous framework can preserve catalytic activity under the air- and moisture-exposed conditions that deactivate the corresponding molecular analogue. Recent studies showing that confinement of metalloradical porphyrins within MOFs can strongly influence active-site reactivity further support this hypothesis.[36,37]

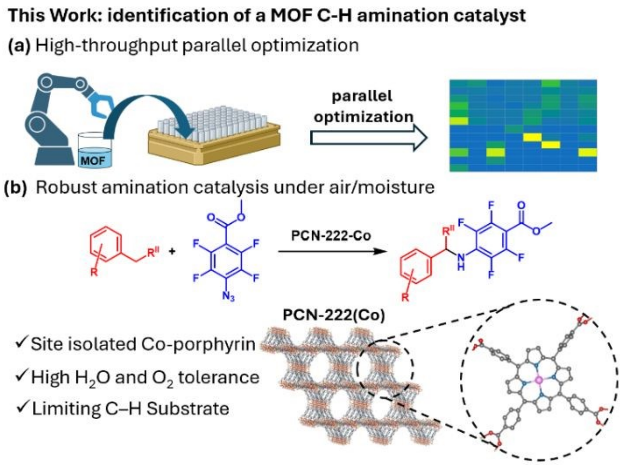

Figure 1. General overview of this work (a) Solution dispersion reactor dosing for high-throughput MOF catalyst assays used in this work and (b) general reaction scheme for the amination reaction in this communication, with a zoomed-out of the Porphyrin linker in PCN-222(Co).

Translating this hypothesis into a practical catalyst platform is not simple. The performance of nitrene-transfer C–H amination catalysts depends strongly on active site microenvironment, azide identity, solvent, and temperature, making it difficult to predict a productive MOF system a priori.[38] High-throughput screening offers an attractive way to identify active catalysts and conditions,[39–41] but applying such workflows to MOF catalysis remains nontrivial. MOFs are

---

[a] Wayne State Department of Chemistry, 5101 Cass Avenue, Detroit, MI 48202, USA. E-mail: bour@wayne.edu.

View Article Online
DOI: 10.1039/D6CC02735K

insoluble, crystalline powders, which are often mechanically unstable.[42] Reliable and non-destructive dosing of sub-milligram quantities without advanced robotics is still a practical barrier to parallel reaction screens. As such, evaluation of MOF catalysts is still often limited to labour-intensive, manually weighed experiments.[39,40]

Here, we report the discovery, optimization, and evaluation of a MOF-based C–H amination catalyst that is highly tolerant of water and oxygen. Using a solution dispersion reactor-dosing workflow to screen reaction conditions (Figure 1a), we identified PCN-222(Co), a mesoporous Zr-based framework containing a cobalt-porphyrin linker, as an effective catalyst for benzylic amination. Under inert, anhydrous conditions, PCN-222(Co) performs similarly to closely related molecular cobalt porphyrins. Under aerobic and moist conditions, however, its behaviour diverges sharply. Whereas the molecular catalysts are largely shut down by O_2 and H_2O, PCN-222(Co) retains high activity. The catalyst also remains effective under limiting C–H substrate conditions and after prolonged benchtop storage.

Catalyst selection and dosing strategy. We selected PCN-222(Co) as the initial candidate for three reasons. First, PCN-222 possesses an isolated porphyrin within a mesoporous (3.7 nm) channel (Figure 1b), which should reduce diffusional penalties that can limit catalysis in primarily microporous catalysts.[43,44] Second, PCN-222 is thermally robust and generally stable to ambient moisture, tolerating aqueous and acidic media.[43,45] Third, the tetra-carboxyphenyl porphyrin (TCPP) linker features a broader ligand environment similar to cobalt tetraphenyl porphyrin (CoTPP)-based catalysts that are widely reported to be effective for C–H amination.

We initially pursued high-throughput evaluation of PCN-222(Co) using our previously reported MOFBead protocol. In this protocol, pulverized MOF is dispersed in glass microbeads and dosed volumetrically to reactors using calibrated scoops.[39] Application of this method to PCN-222(Co), however, produced significant losses in BET surface area (1642 to 549 $m^2\ g^{-1}$) despite maintaining qualitatively similar PXRD patterns (Figures S17, S18 and S15). PCN-222(Co) is apparently insufficiently stable to the mechanical grinding required for this approach. We therefore sought to apply a milder solution dispersion-based dosing protocol similar to that previously reported by Cohen.[40]

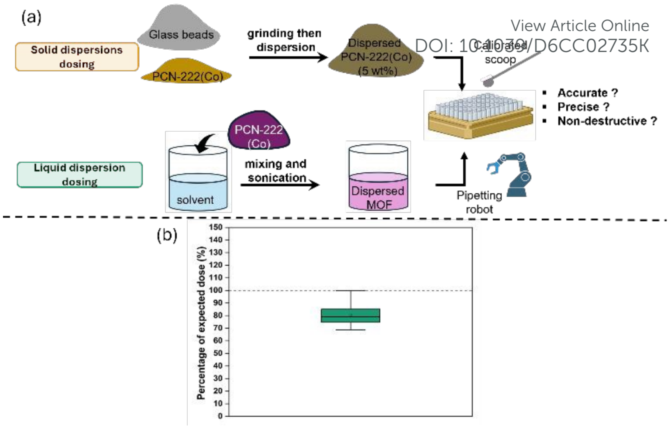

Figure 2. (a) Overview of the two reactor dosing approaches evaluated in this work. (b) Boxplot showing the accuracy and precision of the liquid dispersion loading of PCN-222(Co) into reactor wells a 250 μg/well.

To test the feasibility of solution dispersion dosing techniques, PCN-222(Co) was suspended in THF, sonicated, then pipetted into reactor wells using an automated liquid handling robot. Gas adsorption isotherms and PXRD patterns of solution dispersed MOF confirm that this approach results in less structural degradation than solid dispersion strategies. Figure 2b shows that the surface area was minimally affected by solution-dispersion dosing, as determined by N_2 adsorption isotherms at 77K (1642 to 1606 $m^2\ g^{-1}$). Crystallinity is also maintained, as indicated by PXRD (Figure S15).

Having demonstrated that the MOF maintains its structure using this approach, we next sought to characterize the well-to-well dosing consistency. PCN-222(Co) MOF was dosed into 24 reactor wells, digested in basic DMSO, and the absorbance of each well was measured by plate reader against a calibration curve.[39,46] As shown in figure 2d, dosing precision and accuracy were good at just 250 μg of MOF per well. This method gave a well-to-well dosing coefficient of variation of 10.3%, with an average of 80% of the expected MOF delivered to each well (Figure 2(b)), which is typical for reactor dosing precision in high-throughput chemistry workflows.[47–51] *Reaction optimization.* With a non-destructive reactor dosing strategy in hand, we next carried out a three-dimensional C–H amination activity screen (Figure 3). Four representative azides (Troc-N_3,[52] Tosyl-N_3,[53] Nosyl-N_3,[54] and Fluoro-N_3[55]), six solvents (dichloromethane [DCM], MeCN, 1,4-dioxane, fluorobenzene,

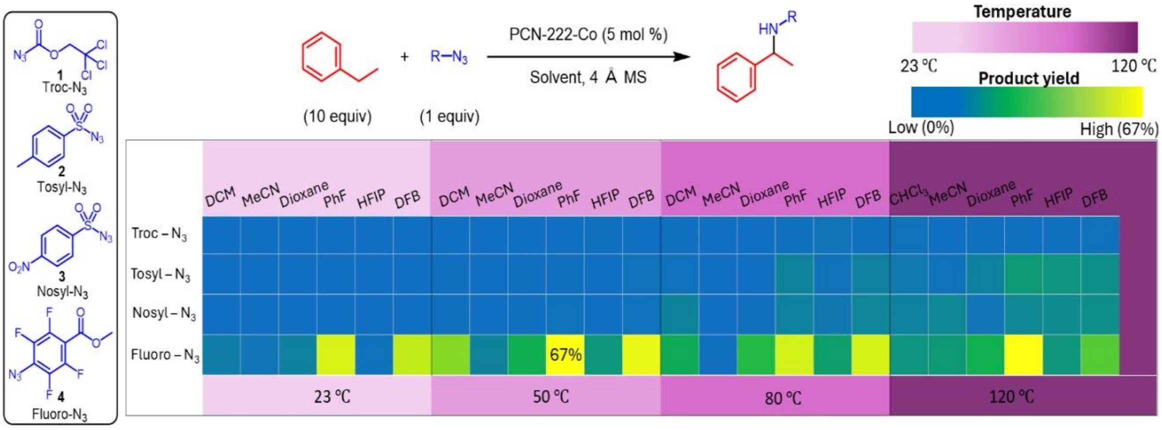

Figure 3. Initial azide, solvent and temperature screen to determine activity. Yield is as determined by GC-MS with high performing conditions confirmed by quantitative NMR. DCM= dichloromethane, MeCN =acetonitrile, Dioxane =1,4-dioxane, PhF = fluorobenzene, DFB = 1,2-difluorobenzene. All reactions were

View Article Online
DOI: 10.1039/D6CC02735K

hexafluoroisopropanol [HFIP], and 1,2-difluorobenzene [DFB]), and four temperatures (23, 50, 80, and 120 °C), using ethylbenzene (10 equiv) as the C–H partner with 5 mol% PCN-222(Co) were evaluated. Approximate yields were determined by GC analysis and higher-yielding conditions were confirmed by NMR spectroscopy against an internal standard. As shown in Figure 3, methyl 4-azido-tetrafluorobenzoate emerged as a uniquely productive azide across all temperatures evaluated. The optimal yield was observed in PhF at 50 °C, giving a ^{19}F NMR yield of 67%. The other azides, Troc-, Tosyl-, and Nosyl-N_3, afforded almost no product until 120 °C. Solvent effects were broadly consistent with trends reported for related transformations.[5–17] Aromatic solvents (PhF, DFB) outperformed other aprotic media. The temperature dependence was weak between 50 and 120 °C (67%, 64%, and 63% by ^{19}F NMR).

Air- and moisture-sensitivity studies. To test if catalyst confinement in the MOF facilitated air and moisture tolerance, we next evaluated the activity of PCN-222(Co) relative to close molecular analogues, Co^{II} tetraphenylporphyrin [Co(TPP)] and Co^{II} tetramethyl carboxyphenyl porphyrin [Co(TMCPP)]. Under N_2, PCN-222(Co), Co(TPP), and Co(TMCPP) catalyze the benzylic amination of ethylbenzene with Fluoro-N_3 at broadly comparable yields (88%, 79%, and 55%, respectively, Figure 4a). However, the activities of the three catalysts under air diverge sharply (Figure 4b). Co(TPP) and Co(TMCPP) both deliver <5% yield, consistent with the established sensitivity of molecular Co-porphyrin amination catalysts to air. The PCN-222(Co) catalyst, in contrast, retains 74% ^{19}F NMR yield under the same open-flask conditions, a loss of only ~14% yield relative to its inert-atmosphere performance. Because Co(TMCPP) bears a similar electronic environment to the framework linker, the divergence between Co(TMCPP) and PCN-222(Co) is consistent with a protective framework microenvironment, rather than a simple electronic effect.

The robustness of the MOF catalyst to water was also investigated. Introduction of 3% v/v H_2O shuts down both molecular catalysts entirely, whereas PCN-222(Co) delivers 69% yield under the same conditions (Figure 4c). Increasing water content incrementally to 100% v/v produces a gradual attenuation of yield but still delivers 58% of the aminated product with water as the only added solvent (Figure 4d). We are cautious about interpreting the high-bulk-water results as a true measure of aqueous catalysis as these reactions were conducted with ten equivalents of ethylbenzene relative to azide. Both reaction partners are likely to partition into the hydrophobic PCN-222 pore, thereby reducing water activity at the active site. Nonetheless, these results demonstrate that the catalyst is overall quite robust to air and water. Consistent with this stability, the catalyst maintained its activity for 10 weeks when stored on the bench (Figure 4e).

Substrate scope. We evaluated the generality of PCN-222(Co)-catalysed benzylic amination across a panel of substrates with benzylic C–H bonds under aerobic conditions (Figure 5), reporting each yield under two stoichiometries: condition A, with the C–H substrate limiting (1.0 equiv) against Fluoro-N_3 (2.0 equiv), relevant to late-stage functionalization of

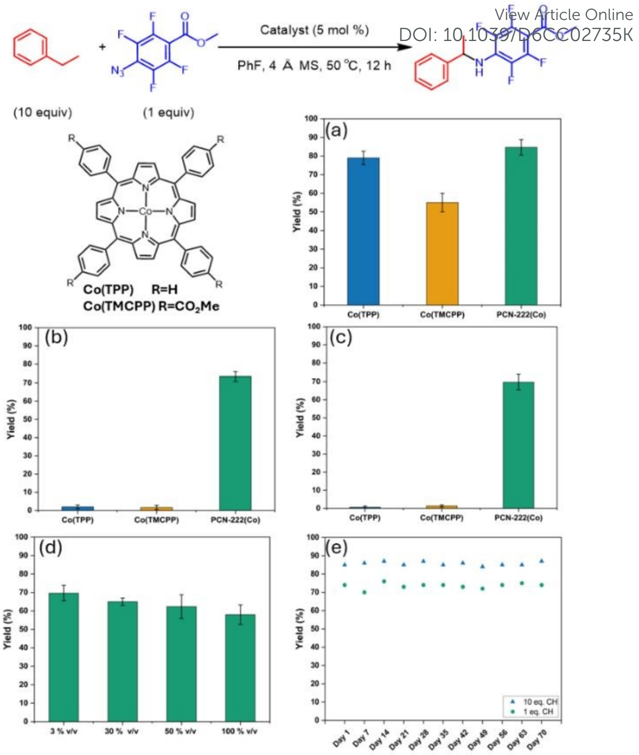

Figure 4. Evaluation of PCN-222(Co) in C–H amination reactions under inert and aerobic environments. Yields are averages of three trials. (a) Comparison to representative molecular catalysts under N_2 atmospheres (b) Comparison to representative molecular catalysts under ambient atmosphere. (c) Comparison of the catalysts with 3% v/v added water. (d) Performance of the PCN-222(Co) with bulk water added. (e) Bench stability time study of the PCN-222(Co) over 70 days.

a valuable substrate; and condition B, with the C–H substrate used as 10 equivalents relative to the azide, which generally gives higher yields. Under both conditions, molecular sieves were used because they boosted yields 5-10% relative to their absence. As shown in figure 5, the catalyst is tolerant of electron rich, neutral and poor substitution patterns. Electron-poor substrates (9-13) performed well with both conditions A and B, yielding moderate to good yields of isolated product. Electron-neutral to slightly rich substrates (14-23) afforded product in good yields as well. Carbocycles with multiple accessible benzylic C–H bonds such as tetrahydronaphthalene and indenes were tolerated under both conditions A and B but with a larger yield gap between A and B than other substrates, potentially due to difunctionalization at the other accessible C–H site. The reaction did not, however, tolerate pyridines or phenolic alcohols (30 and 31).

A notable feature of the MOF-based catalyst is its effectiveness under limiting C–H conditions (condition A). Although condition B delivers higher yields for most substrates, particularly those with multiple accessible benzylic C–H bonds, yields under condition A remain synthetically useful. Practically, this allows the choice between A and B to be determined by which reagent is more valuable, not by catalyst activity limitations. Catalysts that deliver high-yielding C–H amination under limiting C–H conditions remain rare, and in this case the tolerance appears to originate, at least in part, from confinement in the framework. Repeating condition A under N_2

View Article Online
DOI: 10.1039/D6CC02735K

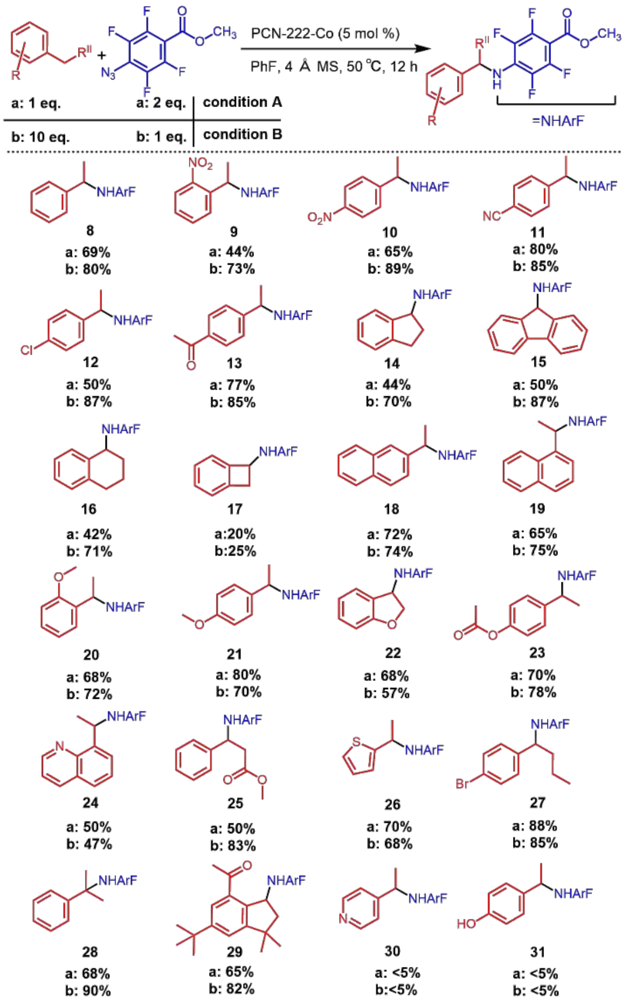

Figure 5. Substrate scope of PCN-222(Co) catalysed reaction under air. Reaction conditions: Fluoro-N_3 (0.12 mmol for condition A, and 0.06 for condition B), benzylic substrate (0.06 mmol for condition A, and 0.6 mmol for condition **B**), PCN-222(Co) (0.003 mmol of Co, 5 mol%), PhF (0.3 mL), molecular sieves (15 mg). All reported yields are isolated yields.

with molecular Co(TPP) gave only 29% yield by ^{19}F NMR, compared with 74% for PCN-222(Co).

In conclusion, this work demonstrates that embedding a Co^{II} porphyrin as the structural linker of the mesoporous MOF PCN-222(Co) confers air and moisture tolerance on a reaction class that is largely restricted to rigorously inert, anhydrous conditions using molecular catalysts. Direct comparison with the electronically similar molecular analogue Co(TMCPP), as well as Co(TPP), argues against a simple linker-electronic origin for this robustness and is instead consistent with a protective framework microenvironment. Although further mechanistic work is needed, we propose that the MOF may limit bimolecular interactions in a manner analogous to bulky peripheral substituents, but without introducing steric crowding at the active site.[56] PCN-222(Co) shows good activity under C–H substrate-limiting conditions and remains active after prolonged bench storage, enhancing its synthetic utility. Together, the stability and activity of the present system suggest that MOFs merit broader consideration as accessible platforms for fine chemical transformations.

Conflicts of interest

There are no conflicts to declare.

Data availability

The data supporting this article have been included as part of the supplementary information (SI). Supplementary information contains supplemental data, experimental details, and characterization data of all new compounds.

Acknowledgements

JCI and JRB thank the National Institutes of Health Grant (R35GM157057) for supporting this research, grant S10OD028488 for NMR instrumentation, and grant R01GM098285-7S1 for mass spectrometry instrumentation. Instrumentation support through the National Science Foundation NSF1427926 (powder X-ray diffraction), NSF0840413 (NMR spectrometer), and NSF2303622 (helium recovery system) is also gratefully acknowledged.

References

1 Y. Park, Y. Kim and S. Chang, *Chem. Rev.*, 2017, **117**, 9247–9301.
2 W. C. P. Tsang, R. H. Munday, G. Brasche, N. Zheng and S. L. Buchwald, *J. Org. Chem.*, 2008, **73**, 7603–7610.
3 W. C. P. Tsang, N. Zheng and S. L. Buchwald, *J. Am. Chem. Soc.*, 2005, **127**, 14560–14561.
4 T. Morofuji, A. Shimizu and J. Yoshida, *J. Am. Chem. Soc.*, 2014, **136**, 4496–4499.
5 H. Lu, V. Subbarayan, J. Tao and X. P. Zhang, *Organometallics*, 2010, **29**, 389–393.
6 H. Lu, H. Jiang, Y. Hu, L. Wojtas and X. P. Zhang, *Chem. Sci.*, 2011, **2**, 2361–2366.
7 F. Ragaini, A. Penoni, E. Gallo, S. Tollari, C. Li Gotti, M. Lapadula, E. Mangioni and S. Cenini, *Chemistry – A European Journal*, 2003, **9**, 249–259.
8 S. Cenini, S. Tollari, A. Penoni and C. Cereda, *Journal of Molecular Catalysis A: Chemical*, 1999, **137**, 135–146.
9 V. Lyaskovskyy, A. I. O. Suarez, H. Lu, H. Jiang, X. P. Zhang and B. De Bruin, *J. Am. Chem. Soc.*, 2011, **133**, 12264–12273.
10 P. Zardi, D. Intrieri, A. Caselli and E. Gallo, *Journal of Organometallic Chemistry*, 2012, **716**, 269–274.
11 M. Goswami, V. Lyaskovskyy, S. R. Domingos, W. J. Buma, S. Woutersen, O. Troeppner, I. Ivanović-Burmazović, H. Lu, X. Cui, X. P. Zhang, E. J. Reijerse, S. DeBeer, M. M. van Schooneveld, F. F. Pfaff, K. Ray and B. de Bruin, *J. Am. Chem. Soc.*, 2015, **137**, 5468–5479.
12 Y. Zhu, W.-C. C. Lee and X. P. Zhang, *J. Am. Chem. Soc.*, 2025, **147**, 15755–15766.
13 K. Lang, Y. Hu, W.-C. C. Lee and X. P. Zhang, *Nat. Synth*, 2022, **1**, 548–557.
14 W.-C. C. Lee and X. P. Zhang, *Angewandte Chemie International Edition*, 2024, **63**, e202320243.
15 K. Lang, S. Torker, L. Wojtas and X. P. Zhang, *J. Am. Chem. Soc.*, 2019, **141**, 12388–12396.
16 A. Caselli, E. Gallo, S. Fantauzzi, S. Morlacchi, F. Ragaini and S. Cenini, *European Journal of Inorganic Chemistry*, 2008, **2008**, 3009–3019.
17 P. F. Kuijpers, M. J. Tiekink, W. B. Breukelaar, D. L. J. Broere, N. P. van Leest, J. I. van der Vlugt, J. N. H. Reek and B. de Bruin, *Chemistry – A European Journal*, 2017, **23**, 7945–7952.
18 F. Ann. Walker, *J. Am. Chem. Soc.*, 1973, **95**, 1154–1159.
19 A. N. Marianov, A. S. Kochubei, T. Roman, O. J. Conquest, C. Stampfl and Y. Jiang, *ACS Catal.*, 2021, **11**, 3715–3729.
20 T. Nakazono, A. R. Parent and K. Sakai, *Chem. Commun.*, 2013, **49**, 6325–6327.
21 M. Goswami, C. Rebreyend and B. De Bruin, *Molecules*, 2016, **21**, 242.
22 W. Zhang, A. Nafady, C. Shan, L. Wojtas, Y.-S. Chen, Q. Cheng, X. P. Zhang and S. Ma, *Angewandte Chemie International Edition*, 2021, **60**, 24312–24317.

23 X.-S. Wang, M. Chrzanowski, C. Kim, W.-Y. Gao, L. Wojtas, Y.-S. Chen, X. P. Zhang and S. Ma, *Chem. Commun.*, 2012, **48**, 7173–7175.

24 L.-H. Xie, M.-M. Xu, X.-M. Liu, M.-J. Zhao and J.-R. Li, *Advanced Science*, 2020, **7**, 1901758.

25 L. Li, Q. Yang, S. Chen, X. Hou, B. Liu, J. Lu and H.-L. Jiang, *Chem. Commun.*, 2017, **53**, 10026–10029.

26 B. R. Reiner, A. A. Kassie and C. R. Wade, *Dalton Trans.*, 2019, **48**, 9588–9595.

27 S. A. Burgess, A. Kassie, S. A. Baranowski, K. J. Fritzsching, K. Schmidt-Rohr, C. M. Brown and C. R. Wade, *J. Am. Chem. Soc.*, 2016, **138**, 1780–1783.

28 V. Piradi, W. Chai, S. K. Emslie, R. E. Sikma, C. Zhang, S. Vasylevskyi, G. Henkelman and S. M. Humphrey, *J. Am. Chem. Soc.*, 2025, **147**, 29119–29129.

29 S. G. Dunning, G. Nandra, A. D. Conn, W. Chai, R. E. Sikma, J. S. Lee, P. Kunal, J. E. Reynolds III, J. Chang, A. Steiner, G. Henkelman, S. M. Humphrey *Angewandte Chemie International Edition* 2018, **57**, 9295–9299.

30 M. M. Pereira, L. D. Dias and M. J. F. Calvete, *ACS Catal.*, 2018, **8**, 10784–10808.

31 S. Fukuzumi, S. Mochizuki and T. Tanaka, *Israel Journal of Chemistry*, 1987, **28**, 29–36.

32 J. Jin, *New J. Chem.*, 2020, **44**, 15362–15368.

33 W.-Y. Gao, M. Chrzanowski and S. Ma, *Chem. Soc. Rev.*, 2014, **43**, 5841–5866.

34 A. Fateeva, P. A. Chater, C. P. Ireland, A. A. Tahir, Y. Z. Khimyak, P. V. Wiper, J. R. Darwent and M. J. Rosseinsky, *Angewandte Chemie International Edition*, 2012, **51**, 7440–7444.

35 L. Zou, R. Sa, H. Lv, H. Zhong and R. Wang, *ChemSusChem*, 2020, **13**, 6124–6140.

36 Z. Qiu, P. C. Bruzzese, Z. Wang, H. Deng, M. Leutzsch, C. Farès, S. Chabbra, F. Neese, A. Schnegg and C. N. Neumann, *J. Am. Chem. Soc.*, 2025, **147**, 12024–12039.

37 Z. Qiu, H. Deng and C. N. Neumann, *Angewandte Chemie International Edition*, 2024, **63**, e202401375.

38 H. Khatua, A. Ghosh, S. Das, S. Patra, S. Nandi and B. Chattopadhyay, *Chem. Rev.*, 2026, **126**, 1145–1205.

39 S. Li, J. C. Izang, J. B. Duque, G. D. Leonard and J. R. Bour, *Inorg. Chem.*, 2026, **65**, 7368–7378.

40 J. M. Palomba, S. P. Harvey, M. Kalaj, B. R. Pimentel, J. B. DeCoste, G. W. Peterson and S. M. Cohen, *ACS Appl. Mater. Interfaces*, 2020, **12**, 14672–14677.

41 K. E. McCullough, D. S. King, S. P. Chheda, M. S. Ferrandon, T. A. Goetjen, Z. H. Syed, T. R. Graham, N. M. Washton, O. K. Farha, L. Gagliardi and M. Delferro, *ACS Cent. Sci.*, 2023, **9**, 266–276.

42 L. R. Redfern and O. K. Farha, *Chem. Sci.*, 2019, **10**, 10666–10679.

43 D. Feng, Z.-Y. Gu, J.-R. Li, H.-L. Jiang, Z. Wei and H.-C. Zhou, *Angewandte Chemie International Edition*, 2012, **51**, 10307–10310.

44 W. Morris, B. Volosskiy, S. Demir, F. Gándara, P. L. McGrier, H. Furukawa, D. Cascio, J. F. Stoddart and O. M. Yaghi, *Inorg. Chem.*, 2012, **51**, 6443–6445.

45 D. Lv, R. Shi, Y. Chen, Y. Chen, H. Wu, X. Zhou, H. Xi, Z. Li and Q. Xia, *Ind. Eng. Chem. Res.*, 2018, **57**, 12215–12224.

46 A. Wang, K. Barcus and S. M. Cohen, *J. Am. Chem. Soc.*, 2023, **145**, 16821–16827.

47 A. C. Impastato, J. T. C. Brown, Y. Wang and N. P. Tu, *ACS Med. Chem. Lett.*, 2023, **14**, 514–520.

48 N. P. Tu and Y. Wang, *RSC Medicinal Chemistry*, 2026, **17**, 52–64.

49 N. J. Gesmundo, N. P. Tu, K. A. Sarris and Y. Wang, *ACS Med. Chem. Lett.*, 2023, **14**, 521–529.

50 J. Meng, C. H. Zhou, L. Yin, J.-A. Chen, J. Xi, C. Chen, T. Cai and Y. Gui, *Mol. Pharmaceutics*, 2025, **22**, 7513–7521.

51 N. P. Tu, A. W. Dombrowski, G. M. Goshu, A. Vasudevan, S. W. Djuric and Y. Wang, *Angewandte Chemie International Edition*, 2019, **58**, 7987–7991.

52 H. Lu, V. Subbarayan, J. Tao and X. P. Zhang, *Organometallics*, 2010, **29**, 389–393.

53 A. I. O. Suarez, H. Jiang, X. P. Zhang and B. de Bruin, *Dalton Trans.*, 2011, **40**, 5697–5705.

54 V. Lyaskovskyy, A. I. O. Suarez, H. Lu, H. Jiang, X. P. Zhang and B. de Bruin, *J. Am. Chem. Soc.*, 2011, **133**, 12264–12273.

55 L.-M. Jin, X. Xu, H. Lu, X. Cui, L. Wojtas and X. P. Zhang, *Angewandte Chemie International Edition*, 2013, **52**, 5309–5313.

56 P. F. Kuijpers, M. J. Tiekink, W. B. Breukelaar, D. L. J. Broere, N. P. van Leest, J. I. van der Vlugt, J. N. H. Reek and B. de Bruin, *Chemistry A European Journal*, 2017, **23**, 7945–7952.

View Article Online
DOI: 10.1039/D6CC02735K

Data availability

The data supporting this article have been included as part of the supplementary information (SI). Supplementary information contains supplemental data, experimental details, and characterization data of all new compounds.